



OPEN Leakage current characteristics in estimating insulator reliability: experimental investigation and analysis

Ali Ahmed Salem^{1✉}, Kwan Yiew Lau^{1✉}, Wan Rahiman^{2✉}, Zulkurnain Abdul-Malek¹, Samir A. Al-Gailani², R. Abd Rahman³ & Salem Al-Ameri¹

The monitoring of leakage current (LC) and voltage characteristics in transmission line insulators is regarded as a good technique for anticipating the physical state of in-service insulators. In the current work, the temporal and frequency characteristics of LC and voltage under various situations were derived for assessing the health condition of porcelain, glass, and silicone rubber insulators. The contamination severity indicated by soluble deposit density, wetting level (Wt), non-soluble deposit density, and uneven pollution distribution (P_u/P_L) were chosen as the environmental factors that impact the insulators. Six criteria were utilized to evaluate the physical state of the insulators, with four of those derived from the LC signal in the time domain, namely, the LC signal peak (C_1), the phase shift between applied voltage and LC (C_2), the LC signal slope between two consecutive peaks (C_3), and the crest factor (C_4). The remaining two indices, namely, the total harmonics distribution (C_5) and the harmonics ratio indicator (C_6), were obtained from the frequency domain of the LC signal. In addition, the flashover voltage index (C_7) was also employed. The LC indicators were then classified based on the laboratory test results to reflect the physical state of the insulators. The findings revealed that the proposed indicators had an important impact in determining the physical state of the insulators. Furthermore, a confusion matrix was created for the test and prediction data using the suggested indicators to determine the effectiveness of each indicator.

One of the important parts of electrical power transmission systems is the transmission line insulators. The efficiency of the transmission systems is related to the health of the insulation systems. Accordingly, it is important to observe different environmental factors, including the type of materials, dampness, and pollutants, that have a considerable influence on the efficiency and health of the high voltage transmission lines insulators that can directly affect the performance of the transmission systems. For example, pollution deposition on the surface of the insulators results in the insulators being subject to a leakage current (LC) flux which leads to extensive discharge activity on the insulators' surface¹⁻⁶. As a result, these discharge activities can escalate and generate a flashover occurrence, which might cause an electrical grid outage or even breakdown⁷⁻⁹. Therefore, it is necessary to monitor and assess the health condition of insulators in order to ensure the integrity of the insulator and the transmission system as a whole^{10,11}. This improves the grid's performance and reduces the likelihood of a malfunction. The scientific community considers the study of the qualities of outdoor insulators and their long-term efficiency to be a relevant topic¹²⁻¹⁵.

There are several advantages of using the LC characteristics as a monitoring strategy. It considers different environmental parameters like surrounding temperature, humidity, pollution, and rainfall¹⁶. Furthermore, LC may be easily monitored online on an ongoing basis. Measuring and analyzing LC has stimulated the interest of many scientists as one of the online tests done on polluted insulators. In addition, the monitoring of LC was performed using a microwave reflectometer system for dry insulator surfaces¹⁷. This form of the monitoring system is however, expensive, making it impractical for power grids. Fontana et al.¹⁸ also introduced a technique

¹Institute of High Voltage and High Current, School of Electrical Engineering, Universiti Teknologi Malaysia, 81310 Johor Bahru, Malaysia. ²School of Electrical and Electronic Engineering, Universiti Sains Malaysia, 14300 Nibong Tebal, Penang, Malaysia. ³Faculty of Electrical and Electronic Engineering, University Tun Hussein Onn Malaysia, 86400 Batu Pahat, Malaysia. ✉email: ahmedali@utm.my; kwanyiew@utm.my; wanrahiman@usm.my

that employed an antenna in LC monitoring on contaminated insulators by capturing the partial discharge electromagnetic radiation. The advantage of this technique is that, unlike other approaches, the parts utilized in it are not destroyed by flashover voltage. Furthermore, some studies in the literature presented different numerical indices for identifying the health condition of insulators, albeit that none of them examined the efficacy of such indicators on high voltage transmission line insulators. Only acoustic and thermal-based diagnostic methods, such as infrared thermal imaging, ultrasonic wave¹⁹, visible light images²⁰, wireless-based system²¹, acoustic fault diagnosis²², network sensors²³, and long-term analysis of LC using optical sensor²⁴, have been used to assess the health of the overhead line insulators.

Moreover, the monitoring of insulator LC under contaminated conditions indicates the capacity to provide a reliable indicator between LC and the condition of high voltage insulators during service. In this regard, many studies have provided various ways of evaluating the physical state of insulators using a particular indication^{16,25–27}. Recently, Palangar²⁸ suggested the use of a combination of two LC harmonic ratios and phase angles to monitor the status of insulators. Although the results of the studies²⁸ provide valuable ways for detecting the status of various types of insulators, estimation of the flashover probability, particularly for composite insulators, is not considered. Meanwhile, Zhao et al.²⁷ employed the LC parameters such as the mean, peak, and standard deviation values to monitor the insulators' state. However, these characteristics were solely employed to calculate the size and density of the contaminated layer over the insulator surface. Another study²⁵ discussed the contaminated insulator's state by measuring the phase angle between the signals of LC and supplied voltage. According to the findings from the literature²⁶, shift angle fluctuation is a good index for evaluating pollution and humidity differences on insulators' surfaces. Other relevant methodologies for predicting insulator pollution incidence include LC components such as the 3rd and 5th odd harmonics, and the total harmonic distortion (THD), which have been used by many researchers^{29–31}. In this approach, the LC signal is analyzed in the frequency domain using the fast Fourier transform (FFT) and wavelet transform. The findings suggest that pollution causes the first and third frequency components, as well as THD³², to grow. In other words, increasing the LC harmonics raises THD, which changes according to the rate of contamination and harmonics of the applied voltage³³.

Having an indicator that reflects the conditions of the insulators^{16,20} is critical. The use of the LC components in frequency and time domains to compute the necessary indicators were provided in the literature³⁴. When calculating flashover occurrences, the indicator 5th/3rd and THD were used. In the case of silicone rubber (SIR) and glass insulators, the extent of pollution and the value of this indicator were shown to be highly correlated. However, disregarding the impacts of the 7th and 9th harmonics components might influence the accuracy of the results that represent the insulator state. Furthermore, a review of the literature revealed that no attempt has been made to analyze the conditions of insulators using index values that take into account the time waveform slope and harmonics up to the 9th component for LC, statistical analysis of the limitations of the indicator as well as a comparison of the performance of these indicators. Therefore, the goal of this research is to create indices based on the characteristics of LC and voltage while considering the major impact of environmental conditions on the performance of three different insulator types, namely porcelain, glass, and SIR. The pollution severity in terms of soluble deposit density (SDD), wetting level (Wt), non-soluble deposit density (NSDD), and non-uniform distribution contamination (P_u/P_L) were taken into consideration as the environmental factors that affect insulators during their service. The indices of LC generated by the impact of these environmental elements were compared. The suggested indicators were evaluated using the confusion matrix for the experimental data and prediction outcomes under 11 kV AC voltage. To sum up, the main contributions of this paper are as follows:

- Perform experimental tests to measure LC and flashover voltage of porcelain, glass, and SIR insulators under different levels of SDD, NSDD, Wt, and P_u/P_L .
- Extracting the characteristics of LC such as peak, harmonics, phase shift angle, slope, and THD.
- Extracting the characteristics of applied voltage such as flashover voltage and withstand voltage.
- Proposing six different indicators based on the characteristics of LC.
- Proposing indicator based on the characteristics of insulator voltage.
- Evaluating the insulator condition using the proposed indicators.
- Statistical evaluation using the confusion matrix between the insulator conditions and prediction conditions based on outcomes of the proposed indicators was performed in order to compare the performance of these indicators.

Method and materials

Test sample. Three types of insulators specimens (porcelain, glass, and SIR) were collected from the transmission lines in Malaysia. The insulators were all naturally field-aged samples with similar aging and service histories. Figure 1 depicts the primary form of the chosen insulators. Table 1 lists the specifications of the insulators.

Experimental setup. The experimental setup was carried out according to the IEC 60,507 standard³⁵ "Artificial pollution tests on high-voltage ceramic and glass insulators to be used in AC systems". All of the trials were conducted in a 50 × 50 × 75 cm test room with polycarbonate sheet walls. Four inlet valves were put in the chamber that was used to moisten the test insulators. Figure 2a shows the schematic diagram for the high voltage insulator experimental setup. Figure 2b depicts a visual representation of the high voltage laboratory's test setup and equipment. The following components made up the experimental circuit setup: A is an energized transformer (230 V/100 kV, 5 kVA, 50 Hz), B is a capacitive voltage divider, C is a test sample, D is a LC monitoring system, E is a steam fog generator and controller, and F is a resistive voltage divider (10,000:1) that is employed to capture the LC data. During the test, the energizing voltage was steadily increased by 2 kV step voltage until it reached 11 kV, and LC was measured at 11 kV. With 11 kV, LC was monitored without interruption under clean,

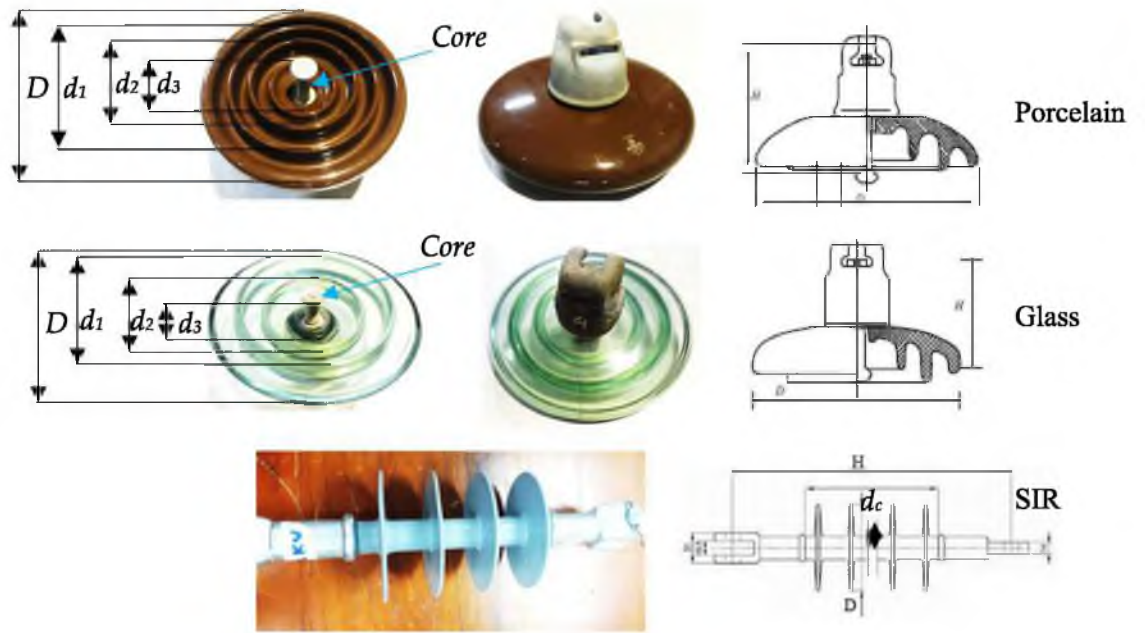


Figure 1. Insulators samples.

Parameter	Symbol	Porcelain	Glass	SIR
Leakage distance	Insulator length	32	34	40
High	H (cm)	14.6	14.6	33
Diameter	D(cm)	25.5	28	10
Rib diameters	d ₁ (cm)	19.5	22.5	–
	d ₂ (cm)	14.5	16	–
	d ₃ (cm)	10.5	8	–
Core diameter	d _c (cm)	5	5	8

Table 1. Insulators parameters.

mild, and medium pollution conditions. Under heavy pollution and wet condition, the step voltage was steadily increased by 1 kV to avoid unintended flashover; under this condition, the discharge activities and the flashover could happen before 11 kV. When a flashover occurred, LC rose sharply to about 10 times the critical current, thus interrupting the voltage supply system.

Pollution and wetting process. Liquid alcohol was used to thoroughly remove traces of oil and grime from all insulators ahead of the experiment. The insulators were then let to dry naturally for one day under the sun’s rays. After that, using the solid layer approach^{36–38}, the contamination was placed on the insulator surface. The SDD was determined using sodium chloride (NaCl) salt while the NSDD was determined using kaolin. 1000 mg of water was used to evenly mix NaCl salt and kaolin uniformly. A conductivity meter was utilized to measure the pollutant solution conductivity at room temperature in order to determine SDD. The SDD was then estimated using Eq. (1) based on the IEC 60507 standard³⁵.

$$SDD = (5.7 \times \sigma_{20})^{1.03} \times V/A \tag{1}$$

where σ_{20} denotes the pollution solution conductivity at 20 °C, V denotes the pollution solution volume, and A is the insulator surface area. Meanwhile, Eq. (2) was used to determine the NSDD.

$$NSDD = ((w_s - w_i) \times 10^3)/A \tag{2}$$

where w_s is the mass of the filter paper under pollution and w_i is the mass of the filter paper in dry conditions. As shown in Table 2, three degrees of SDD and NSDD were assessed in this study, corresponding to light, medium, and high pollution based on the IEC 60,507 standard³⁵. The sample was artificially polluted and hung vertically in the test room for around 24 h to allow it to dry naturally. The test room pressure remained constant throughout the experiment, matching the laboratory’s ambient pressure of about 99.5 kPa. The temperature in the test room was roughly 28 °C, which was about the same as the indoor temperature in Johor, Malaysia. The wetting procedure was carried out using the spray technique. To moisten the tested insulators, eight nozzles were placed

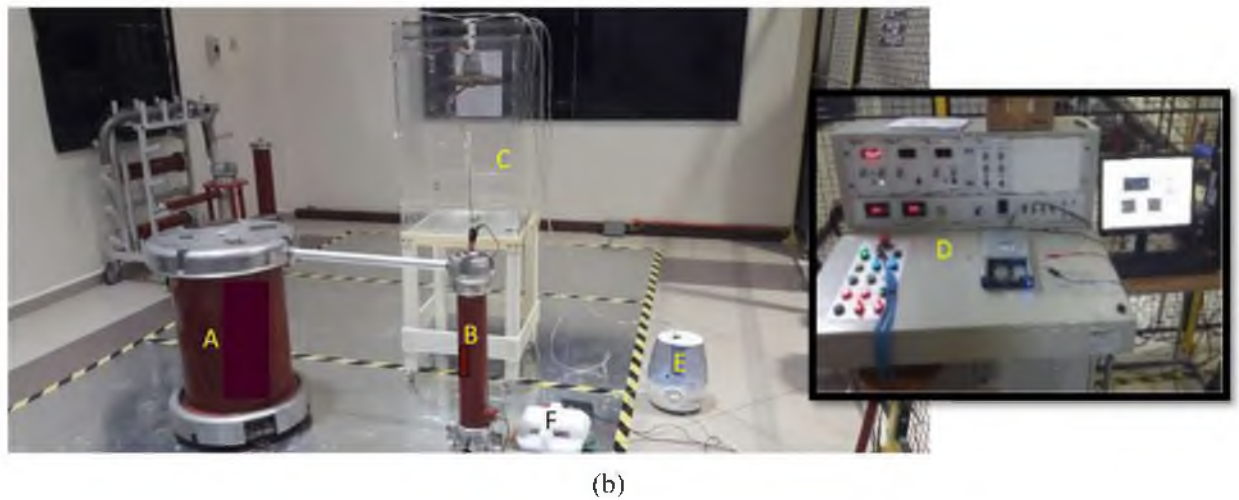
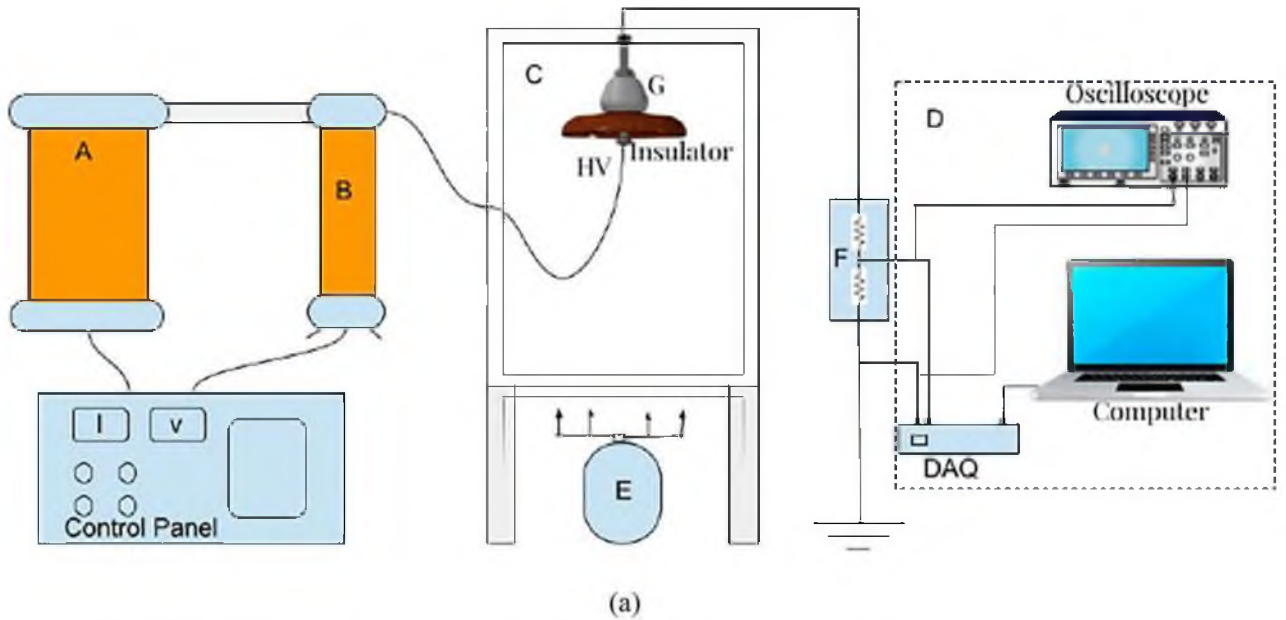


Figure 2. Insulator test: (a) Schematic diagram for experimental setup; (b) Test pictorial view.

Parameters	Values			
σ_{20} (S/m)	0.00	0.39	0.79	1.38
SDD (mg/cm ²)	0.00	0.05	0.12	0.20
NSDD (mg/cm ²)	0.00	0.15	0.25	0.35
Wt (l/h)	0	3	6	9
Contamination level	Clean	Light	Medium	Heavy

Table 2. Pollution severity readings.

around the chamber wall in a regular pattern. The control panel outside the high voltage test cage was in charge of controlling the fog flow rate. The controller was used to manage the wetting rate of the contaminated insulators by adjusting the water flow rate and air pressure. Three levels of wetting rates were employed to mimic the wetting of insulators in different climates: 3 l/h, 6 l/h, and 9 l/h corresponding to low, moderate, and high wetting, respectively³⁹. An issue taken into consideration in choosing the wetting rate between 3 and 9 l/h was the minimum time to wet the sample with no hazard in the pollution layer on the insulator surface.

The insulators were tested under non-uniform and uniform pollutant scenarios. In the case of non-uniform contamination, three distinct contamination ratios of the top to bottom side SDD (P_u/P_l) were chosen: 1/3, 1/5,

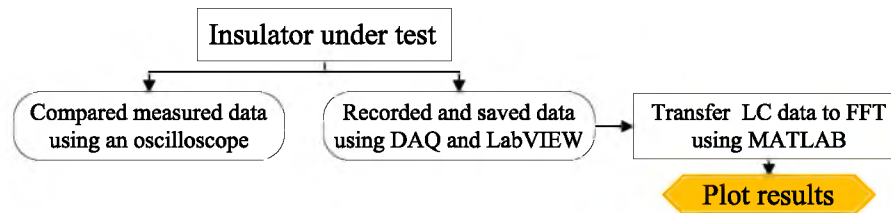


Figure 3. Leakage current monitoring process.

and 1/8. The insulator top and bottom surfaces were polluted separately during the non-uniform application of the contamination layer to generate SDD_1 and SDD_2 , whereas the overall SDD may be met by Eq. (3)^{5,40}:

$$SDD = \frac{SDD_1 \times S_1 + SDD_2 \times S_2}{S_1 + S_2} \quad (3)$$

where S_1 and S_2 are the insulator's upper and lower surface areas, respectively. Based on these specified pollution ratios, the pollution of the upper side SDD_1 and lower side SDD_2 can be satisfied by Eq. (4):

$$SDD_1 = \frac{2 \times SDD}{1 + (P_u/P_L)}, \quad SDD_2 = \frac{2 \times SDD}{1 + (P_u/P_L)} \quad (4)$$

Flashover voltage test. The flashover voltage testing was carried in the test chamber. The flashover voltage was measured using the up-and-down technique. For each contaminated sample, at least 11 tests were done. After passing the first acceptable experiment, the flashover voltage was changed by 5% lower or higher than the prior value in the next ten tests. As a result, the voltage was raised (or decreased) by 2 kV/s increments up (or down) to flashover. In the event of a flashover, the following test was conducted with a 5% lower voltage value; otherwise, the voltage was increased by 5% (after at least 20 s). The average flashover voltage (U_{FO}) and standard deviation (σ) were determined using Eqs. (5 and 6), respectively:

$$U_{FO} = \sum_{i=1}^N U_i / N, \quad N = 11 \quad (5)$$

$$\sigma = \frac{\sqrt{\sum_{i=1}^N (U_i - U_{FO})^2}}{N - 1} \times \frac{100}{U_{FO}} \quad (6)$$

where U_i represents the applied voltage in the i th test and N is the total number of tests.

Monitoring of data. The applied voltage was measured using a capacitive voltage divider via the control panel in the experimental setup as shown in Fig. 2. Meanwhile, the LC monitoring system for LC includes a data acquisition (DAQ) card NI6024E, a computer, and an oscilloscope. A voltage downscaling divider (10,000:1) was employed since the DAQ's input voltage range was just 10 V. The data was sent from the DAQ to the computer, where it was stored as a CSV file and shown in Laboratory Virtual Instrument Engineering Workbench (LabVIEW). The oscilloscope was used to calibrate the DAQ data reading for testing the accuracy of the data reading. Matrix Laboratory (MATLAB) software was used to convert the LC signal in the time domain into the frequency domain. Figure 3 shows the technique used for monitoring and assessing LC.

Characteristic parameter of leakage current. One of the effective ways for developing new techniques for detecting insulators' health is to extract features from LC waveform. These properties may be derived from the frequency and time domains of the LC signal. Six LC characteristics/indicators were extracted in both the time and frequency domains in this work. Figure 4 shows the insulator condition diagnostic diagram utilizing LC characteristics.

Leakage current characteristic in time domain. Four characteristics were chosen in the temporal domain of LC. The peak of LC (I_m) and the phase shift between applied voltage and LC (ϕ) were derived from the general formula of the AC shown in Eq. (7)⁴¹:

$$I = I_m \sin(\omega t + \phi) \quad (7)$$

where ω is angular frequency calculated by, $\omega = 2\pi f$, with the value of frequency f in this study being 50 Hz. So, the first two characteristics can be defined in Eqs. (8) and (9):

$$C_1 = I_m \quad (8)$$

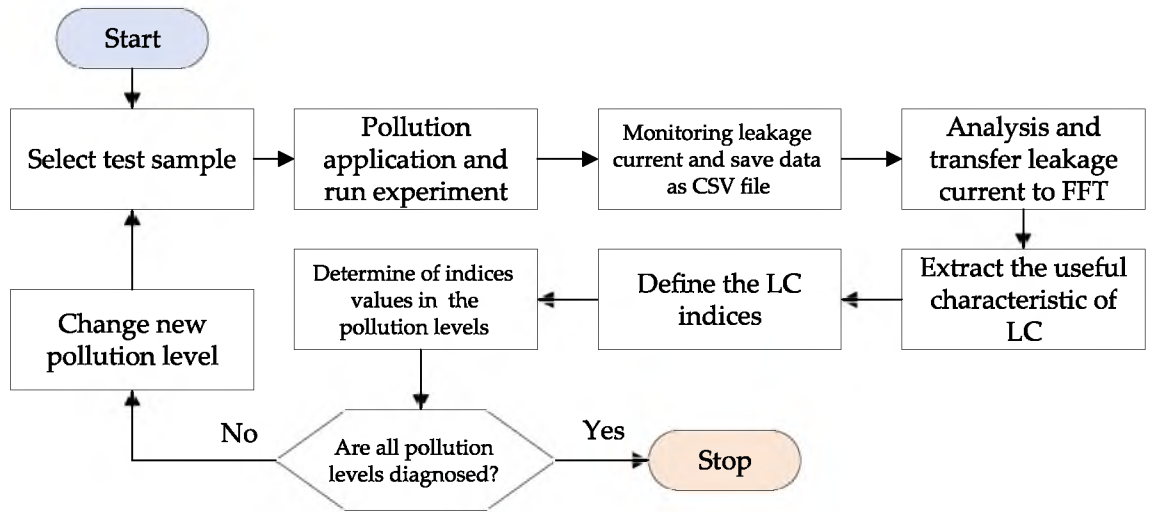


Figure 4. Flowchart process of insulator condition diagnosis.

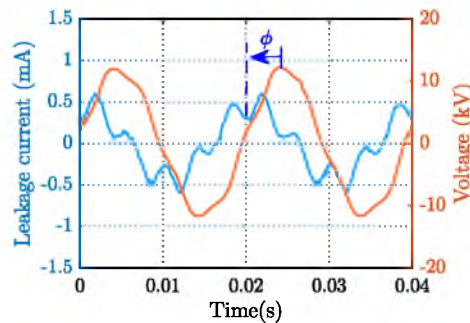


Figure 5. The phase difference between leakage current and applied voltage.

$$C_2 = \phi = \frac{\Delta t}{T} 360^\circ \tag{9}$$

The phase difference between the applied voltage and LC (ϕ), as shown in Fig. 5, was determined using MATLAB software.

Calculating the slope of the line between two successive leakage current signal peaks yielded the third indication C_3 . As a result, Eq. (10) is used to represent C_3 :

$$C_3 = \frac{\sum_{n=1}^m |y_n - y_{n-1}|}{x_n - x_{n-1}} = \frac{\sum_0^m |\Delta y_n|}{\Delta x_n} \tag{10}$$

where Δy_n is the difference in leakage current between neighboring peaks at n , and Δx_n is the time period between these peaks. Figure 6a shows how the LC signal slope was determined. The fourth index was the crest factor (C_4), which was calculated by dividing the peak value by the RMS value of the leakage current (as illustrated in Fig. 6b). As a result, Eq. (11) was used to represent C_4 :

$$C_4 = \frac{I_{peak}}{I_{RMS}} \tag{11}$$

Characteristic of the leakage current in frequency domain. The LC frequency domain at a frequency below 500 Hz for insulators under contamination has characteristic features. Therefore, in this work, the odd harmonics and total harmonic distortion (THD) of LC under 500 Hz were employed to propose indicators for insulators' condition assessment. The LC frequency features were defined by the C_5 (THD) and C_6 (harmonics ratio) indices in Eqs. (12 and 13), respectively:

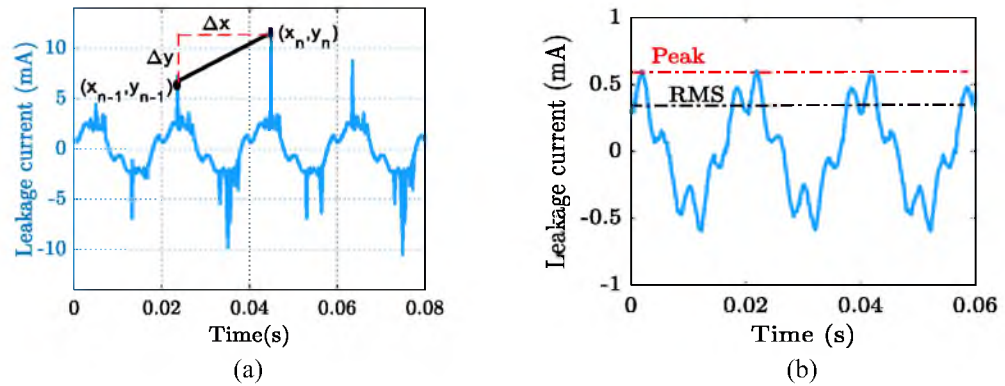


Figure 6. Extracting leakage current characteristics: (a) slope curve, (b) crest factor.

$$C_5 = THD = \frac{\sqrt{\sum_{n=2}^{\infty} I_n^2}}{I_1} \quad (12)$$

$$C_6 = \frac{\sum I_n}{I_3} \quad n = 5, 7, 9 \quad (13)$$

where I_n is the n th order harmonic and n represents the order odd harmonics number.

Flashover voltage indicator. The flashover voltage indicator (C_7) was defined as in Eq. (14):

$$C_7 = \frac{U_{FO} - U_0}{U_0} \quad (14)$$

where U_0 is the flashover voltage under clean conditions, which was measured to be around 53.4 kV for the porcelain insulator, 61.7 kV for the glass insulator and 66 kV for the SIR insulator.

Results and discussion

Leakage current results. Figure 7 depicts the sample of LC results in the time and frequency domains for porcelain, glass, and SIR insulators under different SDD pollution levels, 0.15 mg/cm² of NSDD and 3 l/h of Wt and uniform pollution distribution. Figure 7 illustrates that increasing pollution severity SDD under specific NSDD, Wt, and P_u/P_L causes a large rise in LC. The current spike could be explained by the creation of a layer because of pollution and moisture, which enhanced conductivity along the insulator's surface. Consequently, a path was created to flow LC in the form of ions between insulator poles. Spot-arcing was found on occasion under high pollution conditions, particularly in the presence of moisture. The signal of LC looked to be substantially warped during the arcing activities, as illustrated in Fig. 7d. When LC increased, THD and harmonics levels also increased, but the phase shift angle between LC and voltage decreased. Because the resistive current increased with the constant capacitive current, the phase angle between LC and voltage decreased. Furthermore, a great variance in the odd harmonics 3rd to 9th could be observed when the contamination severity on the surfaces of the insulator was increased gradually, where the third harmonic would increase to overtake other odd harmonics (5th, 7th, and 9th), with a considerable rise in both of the 7th and 9th harmonics, as shown in Fig. 8. It can be noted that when the insulator had an arcing activity on its surface, the 3rd harmonic increased sharply.

Table 3 represents the characteristics of measured LC (I_m , harmonics, THD, and ϕ) of tested insulators under various levels of uniform pollution in Table 2. The LC characteristics under non-uniform pollution distribution are listed in Tables A1–A3 in Appendix A. The 5th and 7th harmonics components were bigger than the 3rd harmonic component in the clean state. Furthermore, this state showed no evidence of flashover. It could be observed that LC rose marginally as the wetting rate increased when the clean insulators were tested under various wetting conditions. This indicates that wetting the insulator surface causes increased charges to flow from the high voltage electrode to the ground electrode. Table 3 shows that LC on a clean insulator surface is very low, approximately 0.183 mA, and that it is primarily capacitive, with a phase change angle of around 90°. Tables A1–A3 in Appendix A demonstrate the effects of P_u/P_L , Wt, and NSDD. Generally, the test findings in Table 3 and Tables A1–A3 indicate that:

- (1) Surface conductivity was lowest in dry circumstances. As a result, raising SDD and NSDD had only a minor influence on LC and its components.
- (2) As the pollution levels SDD and NSDD, as well as the wetting rate, rose, LC increased significantly.
- (3) As SDD, NSDD, and Wt increased and P_u/P_L dropped, LC harmonic amplitudes and THD increased. Meanwhile, ϕ decreased when SDD, NSDD, and Wt rose and P_u/P_L dropped.

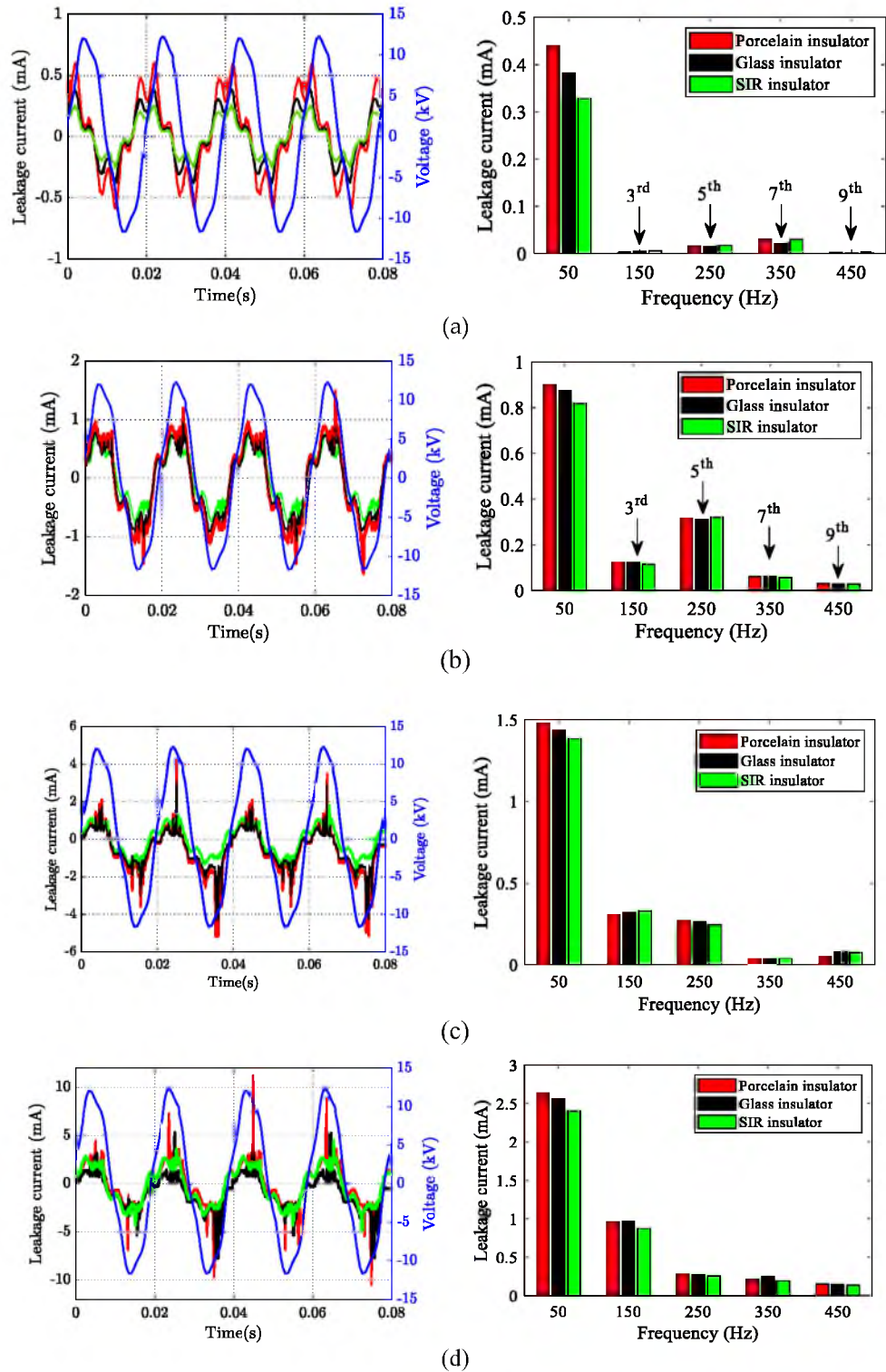


Figure 7. LC waveform and its FFT under different SDD pollution degree, 0.15 of NSDD, and 3 l/h of wetting rate: (a) SDD = 0.00 mg/cm²; (b) SDD = 0.05 mg/cm²; (c) SDD = 0.12 mg/cm²; (d) SDD = 0.2 mg/cm².

Flashover voltage results. The flashover voltage experimental result under different conditions for the tested insulators are listed in Table 4. The flashover voltage as a function of SDD and NSDD under different P_w/P_L for the glass specimen as an example is displayed in Fig. 9a. Meanwhile, Fig. 9b depicts the influence of SDD and wetting rate on the flashover voltage. The findings indicate that the flashover voltage drops significantly

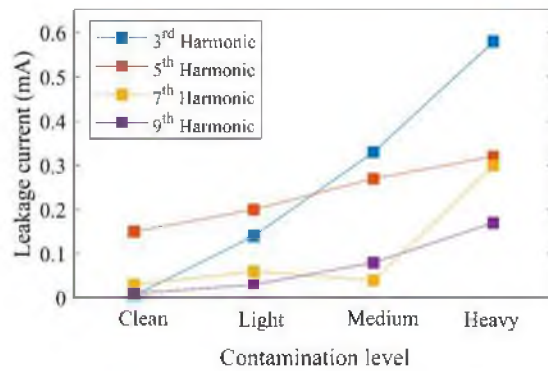


Figure 8. Odd harmonics of leakage current under pollution grading.

with the rising value of the pollution severity/SDD. As the contamination severity increases, the contamination layer's electric conductivity improves. Therefore, the flashover takes place at a lower voltage level. According to the results in Table 4 and Fig. 9, it can be noted that the effect of wetting rate on the flashover voltage is greater than NSDD for the same values of SDD and P_u/P_L .

Leakage current indicators trend under clean condition. As mentioned before, the value of LC changed minorly when the rate of wetting increased on a clean insulator; correspondingly, the LC characteristics would change. Accordingly, the LC indicators of clean insulators under different wetting rates have a slight change as shown in Fig. 9. It can be noted that there is no significant difference between different NSDD in the same wetting rate W_t in the clean condition. Generally, the indicators C_1 , C_3 , C_4 , and C_5 increased with an increase in W_t and NSDD. In a clean state, when W_t increased from 3 to 9 l/h under NSDD of 0.15 mg/cm², C_1 increased from 0.42 to 0.83, C_3 increased from 0.065 to 0.11, C_4 increased from 1.56 to 1.585, and C_5 increased from 0.0028 to 0.0049. On the contrary, the C_2 and C_6 decreased with the rise in NSDD and W_t . When the W_t increased from 3 to 9 l/h under a 0.15 mg/cm² of NSDD, the C_2 decreased from 87.2 to 86.01% and C_6 decreased from 5.9 to 4.7. The slope of increment and decrement under NSDD 0.25 mg/cm² and 0.35 mg/cm² is approximately the same as in the 0.15 mg/cm² with a slight change in the amplitude of indices.

Leakage current indicators trend under various SDD. The SDD has a great effect on the LC indicators. The LC indicators C_1 , C_3 , C_4 , and C_5 rose considerably when SDD increased under any NSDD, W_t , and P_u/P_L while the C_2 and C_6 dropped dramatically as the SDD increased under the same conditions. To show the LC indicators trend under various SDD for porcelain insulator polluted uniformly, Fig. 10 was plotted. In addition, Table 5 illustrates the results of the LC indicators for the porcelain insulator as an example while the LC indicators result for both glass and SIR insulators are listed in Appendix B1 and B2. According to the results in Fig. 10 and Table 5, with C_1 and C_6 taken as an example, under NSDD of 0.25 mg/cm², W_t of 6 l/h and P_u/P_L of 1/1, C_1 corresponded to 1.49, 1.96, and 3.29 mA when SDD was 0.05, 0.12, and 0.2 mg/cm², respectively. It can be observed that the C_1 increased by 10.4% and 15.95% when the SDD increased from 0.05 to 0.12 and 0.2 mg/cm², respectively. Whereas for C_6 , when SDD was 0.05, 0.12 and 0.2 mg/cm², C_6 corresponded to 2.63, 1.09, and 0.56 mA, respectively. It can be said that the direct relationship of insulator surface conductivity with the SDD, which affects the LC signal, is the cause of the large influence on the LC indicators with changes in SDD.

Leakage current indicators trend under different NSDD. The performance of the indices is similar to the previous case with changing NSDD. However, there are discrepancies in the magnitude of increase or decrement. The test results indicated that for constant SDD, W_t , and P_u/P_L , if the NSDD increased, the C_1 , C_3 , C_4 , and C_5 would increase while the C_2 and C_6 would decrease. Figure 11 depicts the C_1 , C_3 , C_4 , C_5 , and C_6 versus NSDD curves for porcelain, glass, and SIR insulators with SDD = 0.2 mg/cm², W_t = 6 l/h, and P_u/P_L = 1/1 to help demonstrate the relationship between NSDD and the suggested indicators.

Leakage current indicators trend under different W_t . Figure 12 shows the connection between the suggested C_1 - C_6 indices and W_t for porcelain, glass, and SIR insulators under SDD = 0.2 mg/cm², NSDD = 0.35 mg/cm², and P_u/P_L = 1/1. It can be seen that when W_t increases, C_2 , and C_6 decreases while the C_1 , C_3 , C_4 , and C_5 increases. For example, when W_t increased from 3 to 6 and 9 l/h with SDD = 0.2 mg/cm², NSDD = 0.35 mg/cm², and P_u/P_L = 1/1, C_1 for porcelain insulator rose by 13.4% and 15.4%, respectively. Meanwhile, C_2 fell by 72.1% and 57.2%, respectively, under identical conditions.

Leakage current indicators trend under different P_u/P_L . Figure 13 shows an example of the relationship between the suggested C_1 - C_6 indices and P_u/P_L for a dirty porcelain insulator with SDD of 0.2 mg/cm², NSDD of 0.35 mg/cm², and W_t of 9 l/h. It can be noted that rising P_u/P_L leads to increased C_2 and C_6 but decreased C_1 , C_3 , C_4 , and C_5 . This suggests that insulators under uniform pollution conditions have a higher probability of flashover occurrence than insulators under non-uniform pollution conditions.

Insulator type			Porcelain			Glass			SIR		
P_u/P_L	NSDD	SDD	Wt								
			3.00	6.00	9.00	3.00	6.00	9.00	3.00	6.00	9.00
1/1	0.15	0.05	24.12	19.61	18.33	25.76	20.95	19.58	28.65	23.29	12.77
		0.12	18.89	15.36	14.35	20.18	16.40	15.33	22.43	18.24	17.05
		0.2	13.81	11.23	10.49	14.75	11.99	11.21	16.40	13.33	12.46
	0.25	0.05	21.97	18.31	16.55	23.46	19.55	17.67	26.09	21.74	19.65
		0.12	17.20	13.80	12.00	18.37	14.74	12.82	20.43	16.39	14.25
		0.2	12.57	10.08	9.02	13.43	10.77	9.63	14.93	11.97	10.71
	0.35	0.05	20.58	16.73	15.64	21.98	17.87	16.70	24.44	19.87	18.57
		0.12	15.52	12.62	11.79	16.57	13.47	12.59	18.43	14.98	14.00
		0.2	11.34	9.22	8.61	12.11	9.84	9.20	13.46	10.94	10.23
1/3	0.15	0.05	26.53	21.57	20.16	28.34	23.04	21.53	31.51	25.62	23.94
		0.12	20.78	16.89	15.79	22.19	18.04	16.86	24.68	20.06	18.75
		0.2	15.19	12.35	11.54	16.22	13.19	12.33	18.04	14.67	13.71
	0.25	0.05	24.16	20.14	17.08	25.80	21.51	18.24	28.69	23.91	20.28
		0.12	18.92	15.18	13.11	20.21	16.22	14.00	22.47	18.03	15.57
		0.2	13.83	11.09	9.83	14.77	11.85	10.50	16.43	13.17	11.67
	0.35	0.05	22.64	18.40	17.20	24.18	19.66	18.37	26.88	21.86	20.43
		0.12	17.07	13.88	12.97	18.23	14.82	13.85	20.27	16.48	15.40
		0.2	12.47	10.14	9.47	13.32	10.83	10.12	14.81	12.04	11.25
1/5	0.15	0.05	28.24	22.96	21.46	30.16	24.52	22.92	33.54	27.27	25.48
		0.12	20.94	17.03	15.91	22.37	18.18	16.99	24.87	20.22	18.90
		0.2	15.55	12.64	11.81	16.61	13.50	12.62	18.47	15.01	14.03
	0.25	0.05	25.72	21.53	18.64	27.46	23.00	19.91	30.54	25.57	22.14
		0.12	19.07	15.81	12.93	20.37	16.89	13.81	22.65	18.78	15.36
		0.2	14.16	11.92	9.91	15.12	12.73	10.58	16.81	14.16	11.77
	0.35	0.05	23.52	19.12	17.87	25.12	20.42	19.08	27.93	22.71	21.22
		0.12	16.82	13.67	12.78	17.96	14.60	13.65	19.97	16.24	15.18
		0.2	12.58	10.23	9.56	13.43	10.92	10.21	14.94	12.15	11.35
1/8	0.15	0.05	30.50	24.80	23.17	32.57	26.48	24.75	36.22	29.45	27.52
		0.12	22.62	18.39	17.19	24.16	19.64	18.35	26.86	21.84	20.41
		0.2	16.79	13.65	12.76	17.93	14.58	13.63	19.94	16.21	15.15
	0.25	0.05	27.77	23.25	19.99	29.66	24.84	21.35	32.98	27.62	23.74
		0.12	20.60	17.08	13.89	22.00	18.24	14.83	24.46	20.28	16.50
		0.2	15.29	12.88	10.62	16.33	13.75	11.35	18.16	15.29	12.62
	0.35	0.05	25.40	20.65	19.30	27.13	22.05	20.61	30.16	24.52	22.92
		0.12	18.16	14.77	13.80	19.40	15.77	14.74	21.57	17.54	16.39
		0.2	13.43	10.06	8.963	15.12	12.31	9.62	16.83	14.28	10.36

Table 4. Flashover experimental results under different conditions for porcelain, glass, and SIR insulators.

the insulator is in an abnormal state. When the flashover voltage indicator value exceeds 0.73, the insulator is in critical condition.

Ranges of indices based on test data. The ranges of the proposed indicators for three insulators (porcelain, glass, and SIR insulators) corresponding to the levels of SDD, NSDD, Wt, and P_u/P_L were categorized in this section based on the LC data. The experimental findings confirmed that C_1 , C_3 , C_4 , C_5 and C_7 levels rose in proportion to increasing SDD, NSDD, and Wt, but decreasing P_u/P_L . Meanwhile, with a rise in SDD, NSDD, and Wt, but a drop in P_u/P_L , C_2 and C_6 declined. Table 6 displays the prediction of insulators conditions ranges based on empirically derived indicators values.

To understand the prediction process of insulator conditions based on the proposed C_1 - C_7 indices, the comparison between the indices values in Table 5 and the boundary condition in Table 6 was performed, as follows:

- (1) The proposed indices values at the normal range were observed in the clean and light pollution cases with Wt less than 4 l/h and NSDD lower than 0.2 mg/cm². In this case, the possibility of discharge occurrence is almost non-existent.
- (2) According to Table 5, the insulator was in abnormal condition under light pollution (0.05 mg/cm²) with heavy wetting Wt (9 l/h) and moderate and heavy levels of NSDD (0.25 and 0.35 mg/cm²) for all contami-

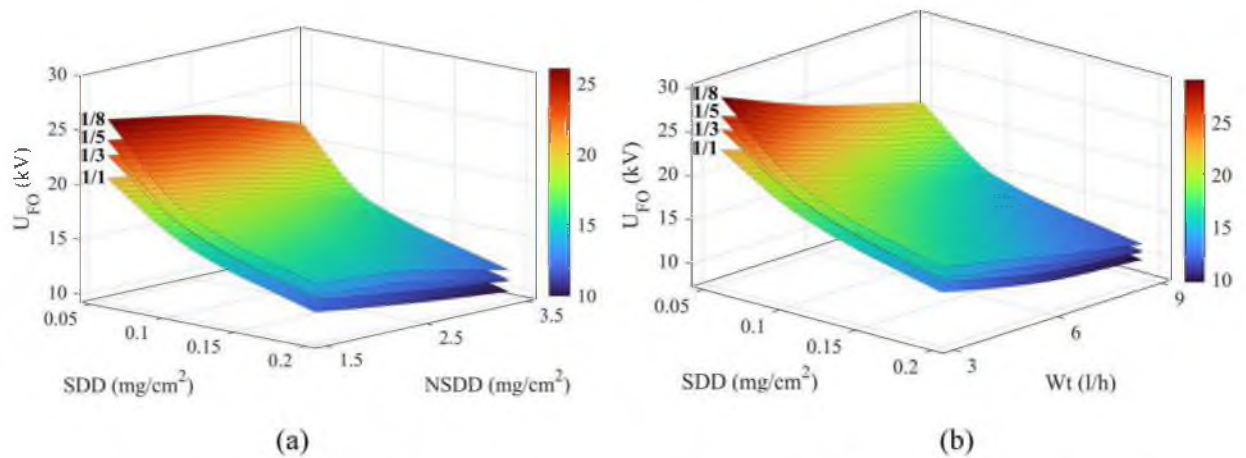


Figure 9. Flashover voltage of glass insulator vs. (a) SDD and NSDD (b) SDD and Wt under different non-uniformity degrees P_u/P_L .

- nation distribution (P_u/P_L) except the 1/8 level. In addition, the insulator under examination displayed an abnormal condition in the presence of moderate pollution (0.12 mg/cm^2) under moderate wetting Wt (6 l/h), NSDD (0.25 mg/cm^2), and all contamination distribution cases; first, in medium contamination condition under Wt (9 l/h), NSDD (0.35 mg/cm^2), and all contamination distribution cases; second, in heavy pollution condition under medium and heavy levels for Wt, NSDD and all pollution distribution cases. The discharge occurring probability in these conditions is high, especially under heavy wet and heavy NSDD.
- (3) The critical condition of the insulator under test was found under two conditions: first, in medium contamination condition under Wt (9 l/h), NSDD (0.35 mg/cm^2), and all contamination distribution cases; second, in heavy pollution condition under medium and heavy levels for Wt, NSDD and all pollution distribution cases. The discharge occurring probability in these conditions is high, especially under heavy wet and heavy NSDD.
 - (4) The insulator must be inspected or cleaned when the values of C_1 , C_3 , C_4 , C_5 , and C_7 indicators are greater than 2.8, 5.1, 2, 45, and 0.73, respectively, and the values for C_2 and C_6 indicators are less than 18.7 and 1, respectively.
 - (5) The indicator values at pre-flashover show that these indicators can also be used to detect the flashover phenomenon for contaminated insulators in operation.

Determination of indices performance. To determine the performance of the proposed indicators precisely, the ability of the indicators to accurately estimate the insulators' state based on 912 tests for three insulators under different conditions was examined. The sensitivity, precision, and accuracy of these indices were calculated using the confusion matrix shown in Fig. 15 during the assessment. The parameters of the confusion matrix were specified based on the insulator condition preparation. The decision of test results and proposed indices are defined as:

- A. The tested insulator condition and the indicator prediction for the insulator condition are positive.
- B. The tested insulator condition is positive, but the indicator prediction for the insulator condition is negative.
- C. The tested insulator condition is negative, but the indicator prediction for the insulator condition is positive.
- D. The tested insulator condition and the indicator prediction for the insulator condition are negative.

Table 7 indicates the positive and negative values for each indicator out of the 912 test samples. The reason for the incorrect predicting findings is either due to a lack of correct application of contaminants on the surface of the insulator or the incorrect indicator diagnosis. The number of prediction results for each indication varied when compared to the total number of test outcomes. The sensitivity, precision, and accuracy results of the proposed indices are shown in Fig. 16.

The difference in the number of expected outcomes may help identify which indicators are the best, with the indices with the most correct anticipated outcomes being the best. In other words, the indices with the greatest number of correct predicted results will be the most accurate.

According to the indices prediction results, C_6 (862) had the highest number of right projected outcomes, followed by C_3 (852), C_7 (851), C_4 (832), C_1 (812), C_5 (801) and C_2 (793). Consequently, C_6 has the best indication accuracy, followed by C_3 , C_4 , C_1 , C_5 , and C_2 (see Table 7). Meanwhile, C_6 has also the highest sensitivity, followed by C_7 , C_4 , C_3 , C_2 , C_1 , and C_5 (see Table 7). Furthermore, the "best" performance is defined as having the smallest fluctuation between sensitivity and specificity⁴². According to Fig. 16, C_6 has the least difference between sensitivity and specificity, followed by C_7 , C_4 , C_3 , C_2 , C_5 , and C_1 .

Leakage current measurement in the practical electric grid. It should be noted that testing the insulators in actual sites differs from typical experimental test setups. Recent studies^{43–45} show that synthetic accelerated tests are used in experimental settings to study flashover states of contaminated insulators. It should

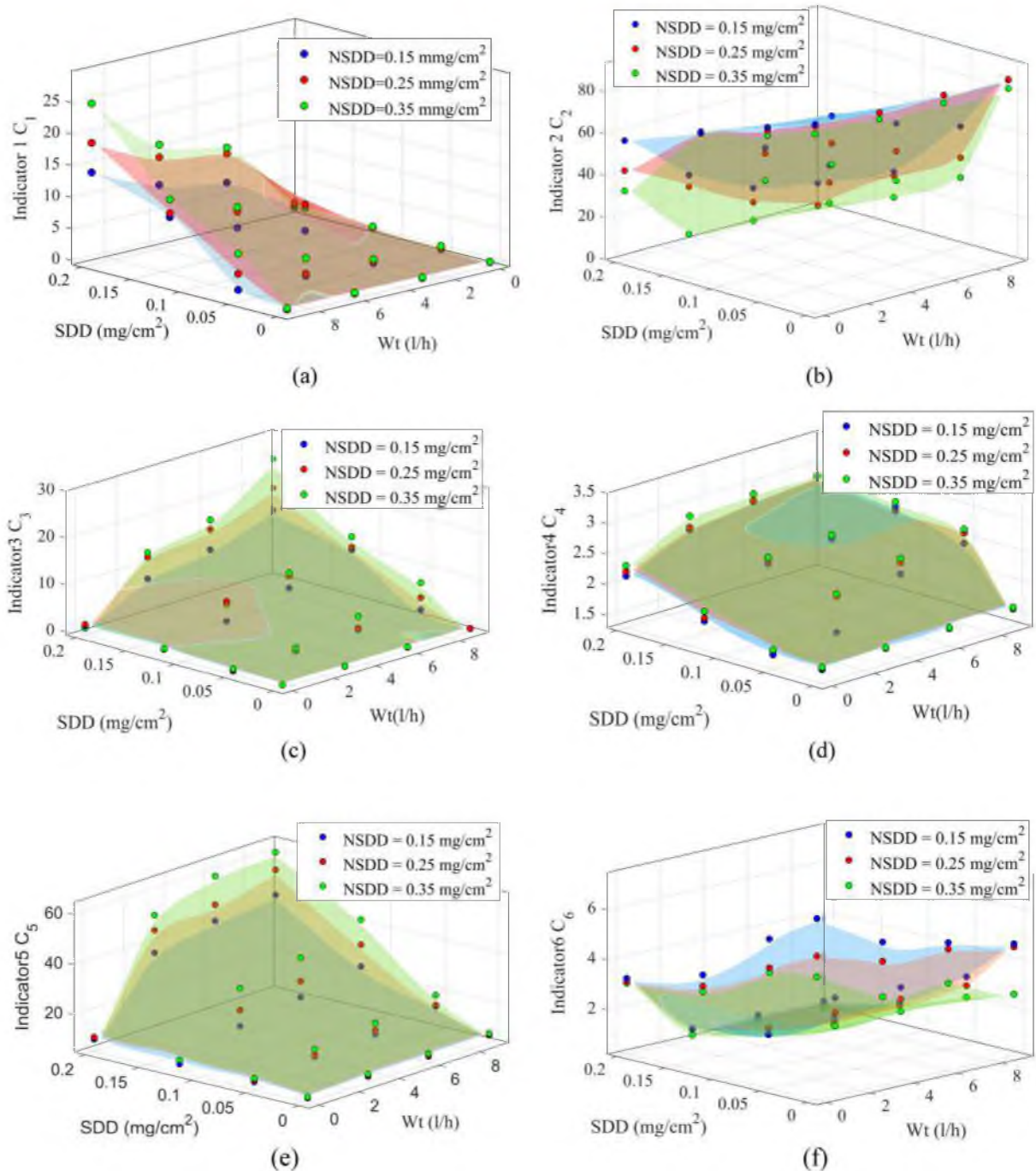


Figure 10. Leakage current indicators of uniform polluted insulators under various Wt and NSDD: (a) C_1 ; (b) C_2 ; (c) C_3 ; (d) C_4 ; (e) C_5 ; (f) C_6 .

be highlighted that all these studies are based on the standard process for insulator tests³⁵. IEC standard³⁵ describes, for example, test types and methods of pre-contamination procedures in an experiment conducted to imitate real on-site pollution situations. Following the standard in the artificial contamination processes should therefore provide test circumstances similar to real on-site contaminated situations, albeit that some variations and inaccuracies between synthetic pollution test conditions and real on-site circumstances (such as noise in voltage and LC signal) are inevitable.

It is noteworthy that the proposed indicators have yet to be tested in real power distribution lines due to the difficulties in accessing real power distribution lines locally. However, effort is currently underway to discuss such a possibility with the local power network provider in accessing a real power distribution line for the purpose of testing the proposed indicators under real operating conditions. Nevertheless, we illustrate in Fig. 17 on how the proposed LC indicators can be used at an on-site power distribution line to predict the condition of contaminated

Pu/PL		1/3						1/5						1/8						
SDD mg/cm ²	NSDD mg/cm ²	W _t l/h	C ₁	C ₂	C ₃	C ₄	C ₅	C ₆	C ₁	C ₂	C ₃	C ₄	C ₅	C ₆	C ₁	C ₂	C ₃	C ₄	C ₅	C ₆
0.05	0.15	0	0.44	88.48	0.15	1.49	8.33	7.27	0.39	90.25	0.14	1.49	8.29	8.80	0.36	90.52	0.14	1.48	8.20	9.39
		3	0.76	85.37	0.39	1.59	10.38	3.57	0.66	87.07	0.38	1.59	10.32	3.69	0.62	87.33	0.38	1.58	10.22	3.89
		6	1.00	72.66	0.82	1.63	11.45	3.32	0.88	74.11	0.80	1.62	11.40	3.50	0.82	74.33	0.80	1.62	11.28	3.67
		9	1.33	62.01	1.08	1.64	14.63	3.18	1.16	63.25	1.07	1.64	14.56	3.21	1.08	63.44	1.06	1.63	14.40	3.61
	0.25	0	0.63	86.91	0.31	1.65	9.03	7.15	0.54	88.66	0.31	1.65	8.99	8.23	0.51	88.92	0.31	1.64	8.89	8.59
		3	1.06	71.27	0.72	1.62	11.05	2.95	0.92	72.69	0.72	1.62	10.99	3.09	0.86	72.91	0.71	1.61	10.88	3.22
		6	1.27	58.39	1.12	1.63	13.04	2.81	1.12	59.57	1.11	1.63	12.97	2.93	1.05	59.74	1.10	1.62	12.83	3.16
		9	1.58	45.92	3.23	1.65	15.25	2.79	1.78	46.84	2.21	1.64	15.17	2.96	1.29	46.97	3.18	1.64	15.02	2.96
	0.35	0	0.77	84.30	0.54	1.66	9.77	6.53	0.68	85.98	0.54	1.66	9.72	7.75	0.63	86.24	0.53	1.65	9.62	8.67
		3	1.39	60.51	0.91	1.63	13.53	2.28	1.21	61.71	0.91	1.62	13.47	2.47	1.13	61.90	0.90	1.62	13.32	2.59
		6	1.73	43.19	3.17	1.64	16.00	2.30	1.52	44.06	3.16	1.64	15.92	2.52	1.41	44.19	3.12	1.63	15.76	2.64
		9	2.23	35.76	5.88	1.65	19.11	2.22	1.93	36.47	5.85	1.65	19.02	2.40	1.81	36.59	5.80	1.65	18.82	2.51
0.12	0.15	0	0.54	76.64	0.66	1.67	8.33	5.58	0.47	78.17	0.65	1.67	8.29	6.57	0.44	78.41	0.65	1.66	8.20	8.23
		3	1.25	59.43	2.35	1.60	15.55	1.36	1.10	60.61	2.34	1.60	15.48	1.69	1.02	60.80	2.32	1.59	15.31	2.04
		6	1.39	41.48	4.90	1.66	19.15	1.39	1.21	42.30	4.88	1.65	19.06	1.57	1.13	42.43	4.83	1.65	18.86	1.76
		9	1.64	29.23	8.45	2.32	23.59	1.55	1.43	29.81	8.40	2.32	23.47	1.60	1.34	29.91	8.33	2.31	23.23	1.79
	0.25	0	0.62	81.69	0.82	2.53	10.02	5.29	0.53	83.32	0.82	2.53	9.97	5.99	0.50	83.57	0.80	2.52	9.86	7.68
		3	1.41	56.53	5.88	1.67	22.06	1.50	1.23	57.66	5.85	1.67	21.95	1.63	1.15	57.83	5.80	1.66	21.72	1.71
		6	1.61	32.53	7.05	2.27	25.61	1.37	1.40	33.18	7.01	2.27	25.49	1.55	1.31	33.27	6.95	2.26	25.23	1.62
		9	1.83	27.03	8.97	2.52	32.44	1.37	1.60	27.58	8.91	2.52	32.28	1.63	1.49	27.66	8.83	2.51	31.94	1.67
	0.35	0	0.79	75.80	0.83	2.70	10.05	4.35	0.69	77.32	0.83	2.70	10.00	4.91	0.65	77.56	0.82	2.69	9.90	6.17
		3	1.67	42.69	5.38	1.69	30.95	1.21	1.46	43.55	5.36	1.68	30.80	1.43	1.36	43.67	5.31	1.68	30.48	1.52
		6	1.72	22.21	7.68	2.31	35.13	1.21	1.50	22.65	7.64	2.31	34.96	1.34	1.40	22.72	7.57	2.30	34.59	1.59
		9	2.20	16.09	10.82	2.59	42.66	1.25	1.92	16.42	10.75	2.59	42.44	1.29	1.80	16.46	10.66	2.58	42.00	1.47
0.2	0.15	0	0.71	61.18	1.08	2.77	10.06	3.57	0.60	62.41	1.07	2.76	10.01	3.95	0.56	62.60	1.06	2.75	9.91	4.93
		3	2.24	34.57	6.14	1.84	37.10	0.70	1.94	35.27	6.11	1.84	36.91	0.79	1.82	35.37	6.05	1.84	36.52	0.95
		6	2.49	18.92	7.97	2.49	41.93	0.66	2.16	19.30	7.92	2.49	41.72	0.69	2.03	19.35	7.85	2.48	41.28	0.83
		9	3.08	12.45	11.78	2.62	44.41	0.63	2.69	12.69	11.71	2.62	44.18	0.60	2.52	12.73	11.60	2.61	43.72	0.75
	0.25	0	0.87	45.79	1.32	2.82	10.94	3.43	0.76	46.70	1.32	2.81	10.88	3.74	0.71	46.85	1.30	2.80	10.76	4.50
		3	2.48	28.47	9.99	1.90	46.29	0.74	2.16	29.04	9.94	1.89	46.06	0.75	2.02	29.12	9.84	1.89	45.58	0.79
		6	2.78	11.55	11.67	2.57	48.54	0.66	2.42	11.78	11.60	2.56	48.30	0.74	2.27	11.82	11.50	2.55	47.79	0.74
		9	3.38	1.12	15.73	2.58	54.57	0.56	2.94	1.14	15.63	2.58	54.30	0.61	2.75	1.15	15.49	2.57	53.73	0.68
	0.35	0	0.91	35.35	0.66	2.75	10.78	3.35	0.78	36.05	0.66	2.75	10.73	3.64	0.74	36.17	0.65	2.73	10.62	4.23
		3	3.19	4.22	10.83	2.02	52.43	0.59	2.92	4.31	10.76	2.01	52.17	0.67	1.75	4.32	10.66	2.01	51.61	0.82
		6	4.83	2.23	13.34	2.60	60.15	0.70	3.44	2.27	13.27	2.60	59.86	0.60	2.24	2.28	13.15	2.59	59.23	0.70
		9	5.51	0.00	20.96	2.66	61.75	0.48	4.80	0.00	19.80	2.65	61.44	0.55	4.48	0.00	17.51	2.64	60.80	0.63

Table 5. LC indicators under various SDD, wetting rate W_t and NSDD for non-uniform polluted porcelain insulator. Significant values are in [bold].

insulators. The ground electrode of the glass insulator on a 11 kV distribution line can be connected to a resistive divider and subsequently to an oscilloscope for signal reading.

Conclusions

To effectively analyse the stability of contaminated insulators, this article conducted an experimental analysis of leakage current indices. The contamination, wetting rate, non-soluble deposit density, and non-uniform distribution pollution were all studied and executed on the porcelain, glass, and SIR insulators. Then, based on the laboratory test results, the time and frequency characteristics of the leakage current and flashover voltage were extracted and employed as assessment indicators for the insulators' physical conditions. The ranges of the leakage current indicators for four different insulators' conditions were classified. The confusion matrix technique was used for assessing the performance of the proposed indicator. The indicators are all relevant in detecting the condition of contaminated insulators. The C₆, C₃, and C₄ indicators perform better than other indicators in

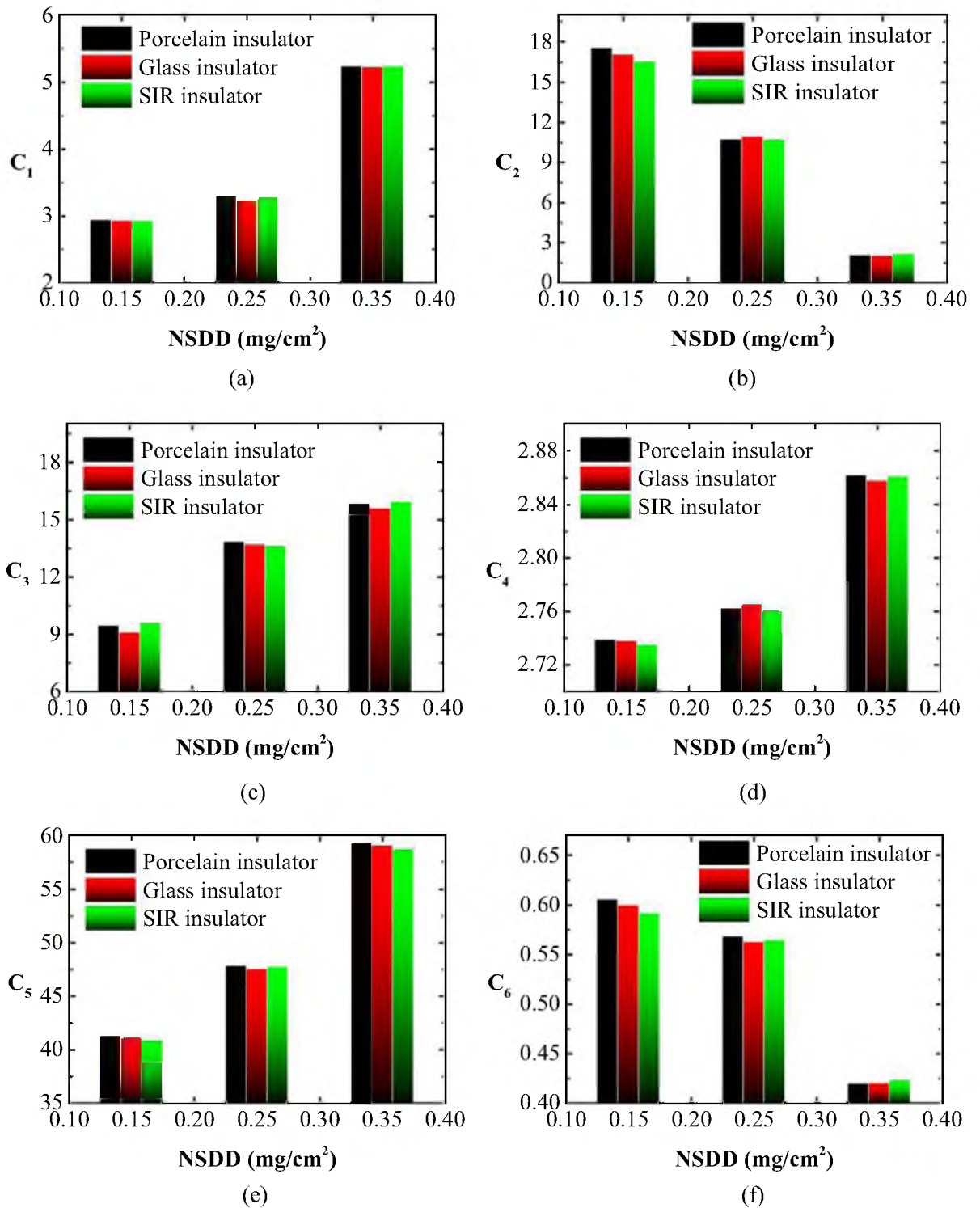


Figure 11. LC indicators versus NSDD for tested insulators under SDD = 0.2 mg/cm², Wt = 9 l/h and P_v/P_L = 1/1: (a) C₁; (b) C₂; (c) C₃; (d) C₄; (e) C₅; (f) C₆.

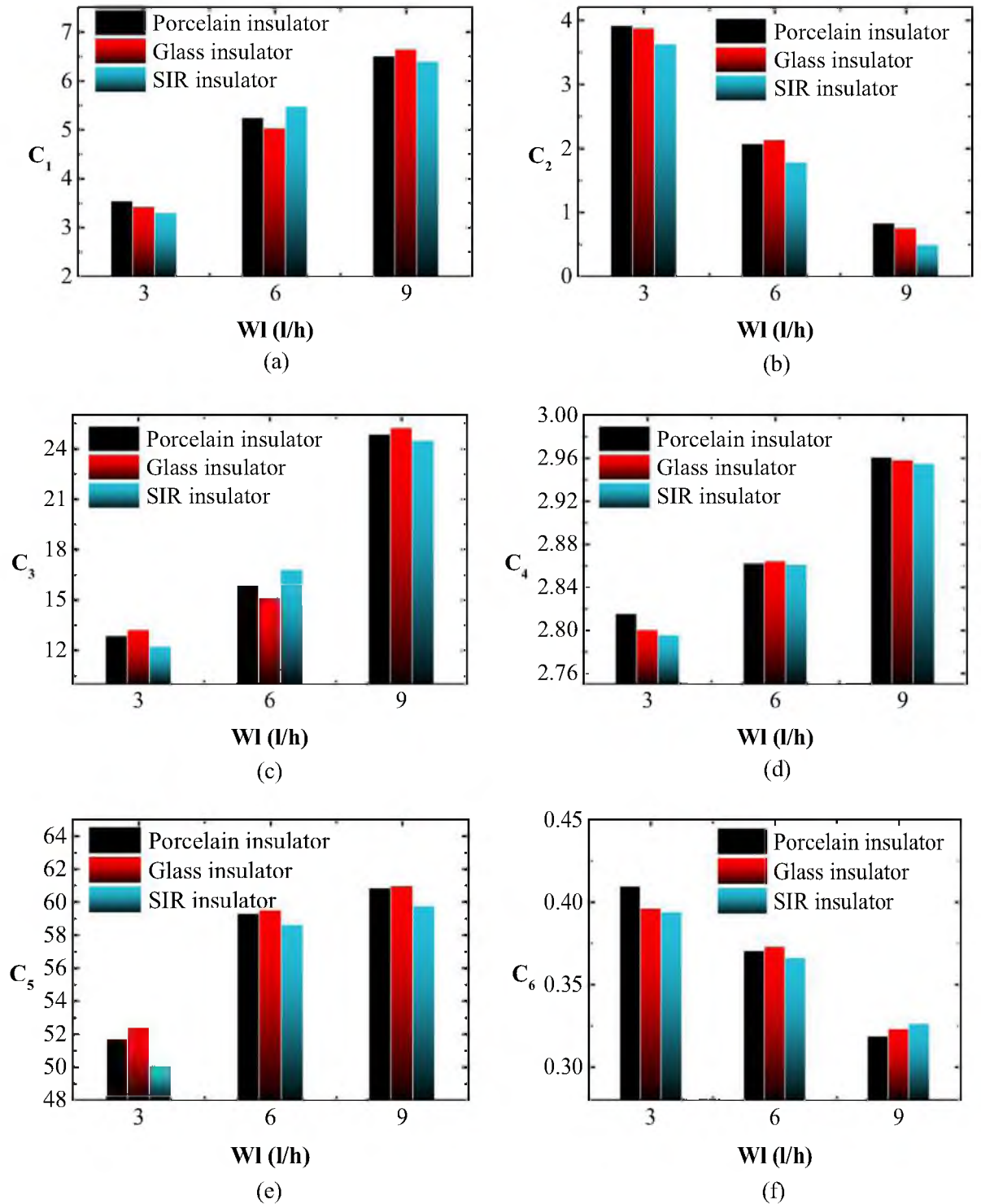


Figure 12. LC indicators versus Wt for tested insulators under $SDD=0.2 \text{ mg/cm}^2$, $NSDD=0.35 \text{ mg/cm}^2$ and $P_w/P_L=1/1$: **(a)** C_1 ; **(b)** C_2 ; **(c)** C_3 ; **(d)** C_4 ; **(e)** C_5 ; **(f)** C_6 .

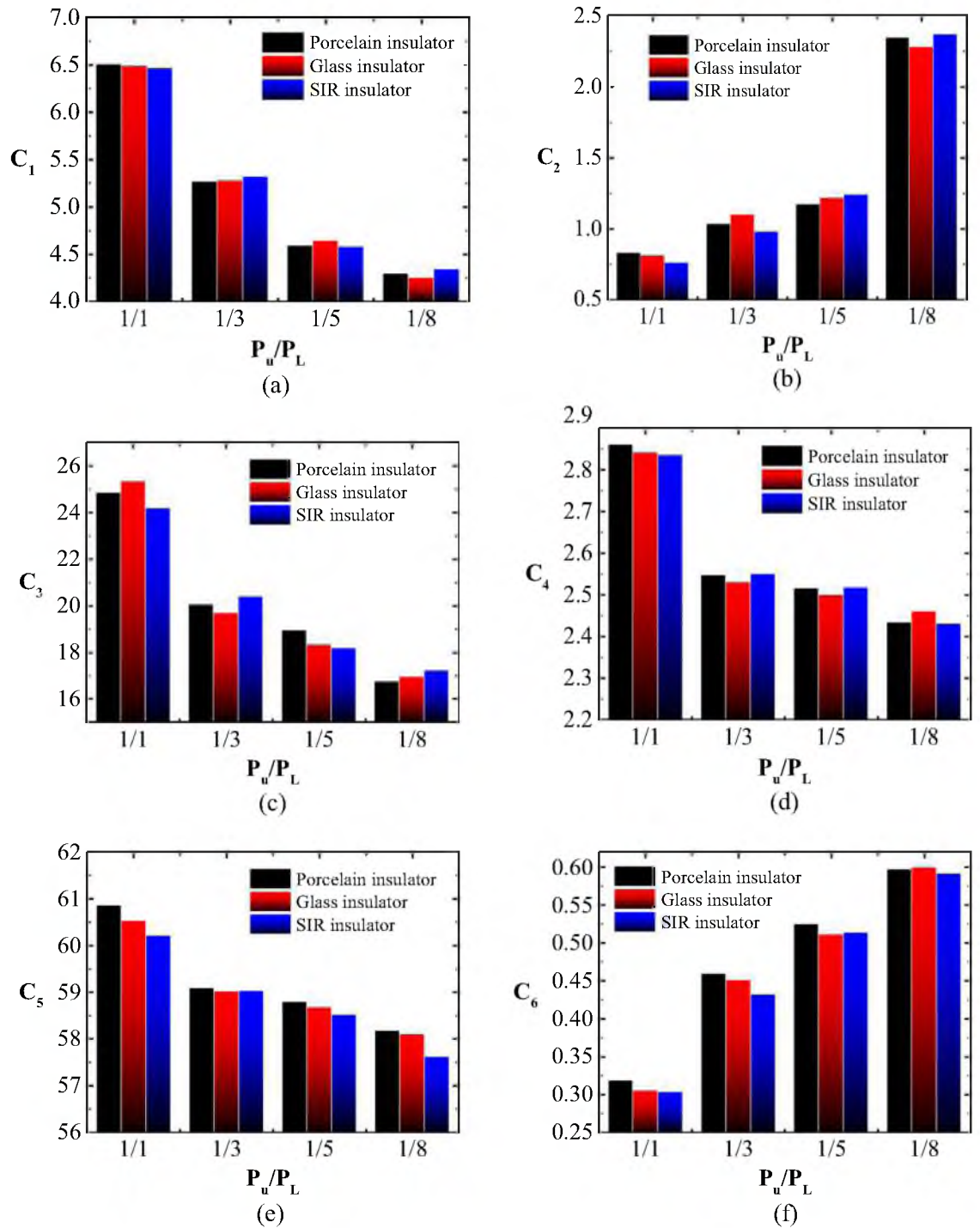


Figure 13. LC indicators versus P_u/P_L for tested insulators under SDD = 0.2 mg/cm², NSDD = 0.35 mg/cm² and Wt = 9 l/h: (a) C₁; (b) C₂; (c) C₃; (d) C₄; (e) C₅; (f) C₆.

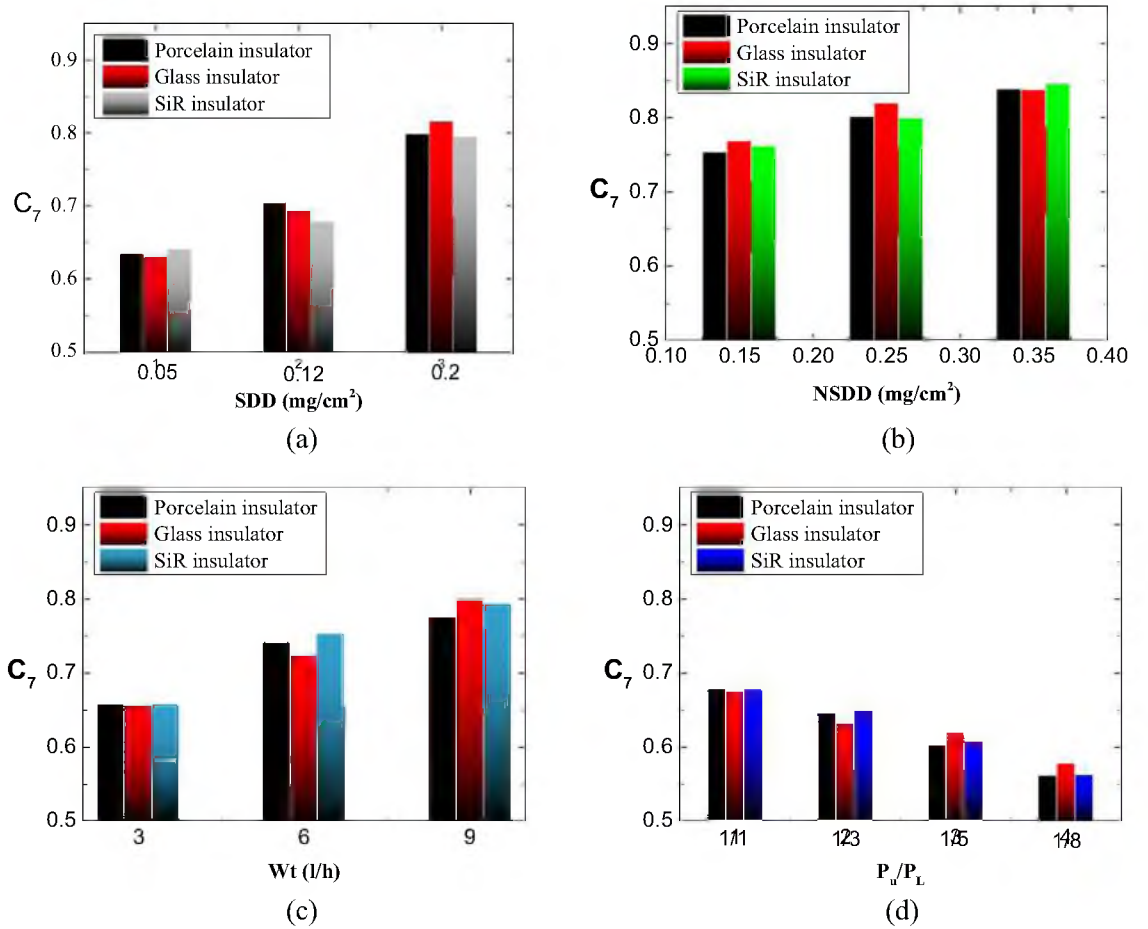


Figure 14. Flashover voltage indicator under different: (a) SDD; (b) NSDD; (c) Wt; (d) P_u/P_L .

Indicator	Normal range	Abnormal range	Critical range	Pre-flashover value
C_1	< 1.165	> 1.165 and < 2.86	> 2.86	> 10
C_2	> 59.3	> 18.7 and < 59.3	< 18.7	≈ 0
C_3	< 1.53	> 1.53 and < 5.1	> 5.1	> 28
C_4	< 1.6	> 1.6 and < 2	> 2	> 2.8
C_5	< 15	> 15 and < 45	> 45	> 65
C_6	> 3	> 1 and < 3	< 1	< 0.4
C_7	< 0.62	> 0.62 and < 0.73	> 0.73	> 0.85

Table 6. Insulator condition dependent on experimentally determined indicators values.

terms of accuracy, with 0.950, 0.935, and 0.923, respectively, according to the confusion matrix analysis. Future research directions linked to the diagnosis of the insulator condition can include, but are not limited to, the following work: (1) testing the proposed indicators in real power distribution lines; (2) designing a device capable of directly detecting the state of the insulator and wirelessly transferring the data based on the proposed indicators in this work; and (3) developing a new optimization technique to denoise and classify the signal captured directly from the transmission line based on the insulator’s conditions.

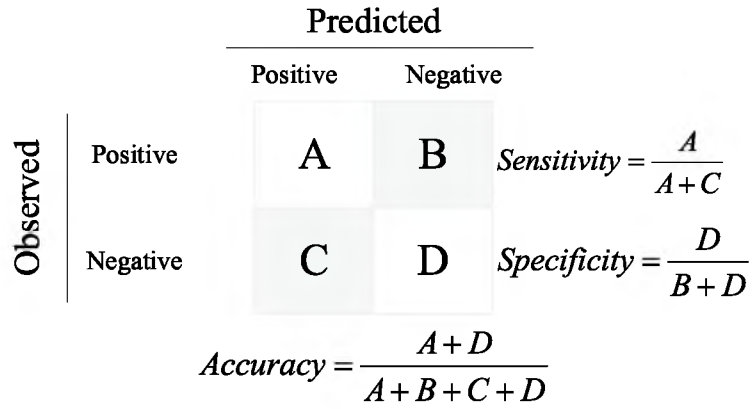


Figure 15. Confusion matrix for determining indices' sensitivity, specificity, and accuracy.

Indicator	A	B	C	D	Sensitivity	Specificity	Accuracy
C ₁	812	62	39	23	0.954	0.271	0.892
C ₂	793	66	45	32	0.946	0.327	0.881
C ₃	852	34	27	23	0.969	0.404	0.935
C ₄	832	43	29	32	0.966	0.427	0.923
C ₅	801	64	44	27	0.948	0.297	0.885
C ₆	862	23	24	27	0.973	0.540	0.950
C ₇	851	35	26	24	0.965	0.477	0.918

Table 7. The indices' sensitivity, specificity, and accuracy for the 936 tests.

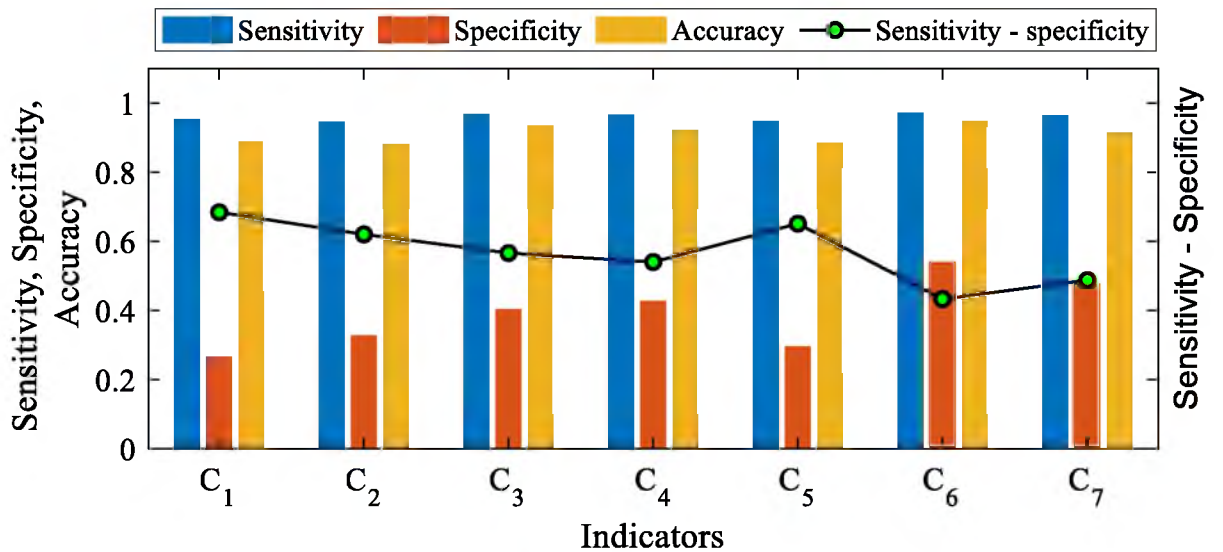


Figure 16. The indicators sensitivity, specificity, accuracy, and the difference between sensitivity and specificity.

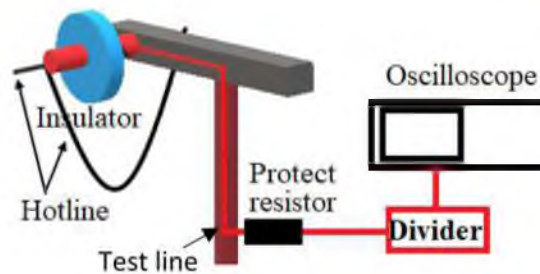


Figure 17. Illustration of on-site insulator testing.

Data availability

All data generated or analyzed during this study were included at <https://github.com/Salem1985-dot/ali.git>. All data in this work has been obtained from the insulators test in a high voltage laboratory, Universiti Teknologi Malaysia (UTM), Johor Bahru, Malaysia.

Received: 27 July 2021; Accepted: 31 July 2022

Published online: 02 September 2022

References

- Sopelsa Neto, N. F. *et al.* A study of multilayer perceptron networks applied to classification of ceramic insulators using ultrasound. *Appl. Sci.* **11**, 1592 (2021).
- Salem, A. A. *et al.* Risk assessment of polluted glass insulator using leakage current index under different operating conditions. *IEEE Access* **8**, 175827–175839 (2020).
- Lan, L. *et al.* Studies on metallurgical contamination accumulation characteristics on ceramic insulator of 500 kV AC transmission line. *IET Sci. Meas. Technol.* **13**, 722–728 (2019).
- Zhang, D. *et al.* Research on the non-contact pollution monitoring method of composite insulator based on space electric field. *Energies* **14**, 2116 (2021).
- Zhang, Z. *et al.* DC flashover dynamic model of post insulator under non-uniform pollution between windward and leeward sides. *Energies* **12**, 2345 (2019).
- Liu, Y., Li, Q., Du, B. & Farzaneh, M. Feature extraction and classification of surface discharges on an ice-covered insulator string during AC flashover using gray-level co-occurrence matrix. *Sci. Rep.* **11**, 2542 (2021).
- Mestriner, D. & Brignone, M. Corona effect influence on the lightning performance of overhead distribution lines. *Appl. Sci.* **10**, 4902 (2020).
- Yamashita, T., Ishimoto, R. & Furusato, T. Influence of series resistance on dry-band discharge characteristics on wet polluted insulators. *IEEE Trans. Dielectr. Electr. Insul.* **25**, 154–161 (2018).
- Ren, A., Liu, H., Wei, J. & Li, Q. Natural contamination and surface flashover on silicone rubber surface under haze-fog environment. *Energies* **10**, 1580 (2017).
- De Barros Bezerra, J. M., Lima, A. M. N., Deep, G. S. & da Costa, E. G. An evaluation of alternative techniques for monitoring insulator pollution. *IEEE Trans. Power Deliv.* **24**, 1773–1780 (2009).
- Choi, I. H. *et al.* Damage evaluation of porcelain insulators with 154 kV transmission lines by various support vector machine (SVM) and ensemble methods using frequency response data. *Appl. Sci.* **10**, 84 (2020).
- Suda, T. Frequency characteristics of leakage current waveforms of artificially polluted suspension insulators. *IEEE Trans. Dielectr. Electr. Insul.* **8**, 705–709 (2005).
- Hussain, M. M., Farokhi, S., McMeekin, S. G. & Farzaneh, M. Risk assessment of failure of outdoor high voltage polluted insulators under combined stresses near shoreline. *Energies* **10**, 1661 (2017).
- Fofana, I. *et al.* Lessons to learn from post-installation pollution levels assessment of some distribution insulators. *Energies* **13**, 4064 (2020).
- Chen, W., Wang, W., Xia, Q., Luo, B. & Li, L. Insulator contamination forecasting based on fractal analysis of leakage current. *Energies* **5**, 2594–2607 (2012).
- Salem, A. A. *et al.* The leakage current components as a diagnostic tool to estimate contamination level on high voltage insulators. *IEEE Access* **8**, 92514–92528 (2020).
- Jiang, Y. *et al.* Monitoring contamination level on insulator materials under dry condition with a microwave reflectometer. *IEEE Trans. Dielectr. Electr. Insul.* **23**, 1427–1434 (2016).
- Fontana, E. *et al.* Sensor network for monitoring the state of pollution of high-voltage insulators via satellite. *IEEE Trans. Power Delivery* **27**, 953–962 (2012).
- Park, K.-C. & Yoon, J. R. Analysis of the insulators' radiation noises for error detections. *Proc. Symp. Ultrason. Electron.* **30**, 249–250 (2009).
- Jin, L., Tian, Z., Ai, J., Zhang, Y. & Gao, K. Condition evaluation of the contaminated insulators by visible light images assisted with infrared information. *IEEE Trans. Instrum. Meas.* **67**(6), 1349–1358 (2018).
- Upadhyay, A. K., Johri, P., Reddy, C. C. & Sandhu, A. Direct measurement of accumulated space charge using external currents. *IEEE Trans. Instrum. Meas.* **70**, 1–8 (2021).
- Park, K.-C., Motai, Y. & Yoon, J. R. Acoustic fault detection technique for high-power insulators. *IEEE Trans. Ind. Electron.* **64**, 9699–9708 (2017).
- Fontana, E. *et al.* Sensor network for monitoring the state of pollution of high-voltage insulators via satellite. *IEEE Trans. Power Del.* **27**, 953–962 (2012).
- Silva, L. H. S., Oliveira, S. C., Lima, R. A. D. & Fontana, E. Long term analysis of leakage current pulses registered by an optical sensor network. in *IEEE MTT-S Int. Microw. Symp. Dig.*, 1–5 (2013).
- Douar, M. A., Mekhalidi, A. & Bouzidi, M. C. Flashover process and frequency analysis of the leakage current on insulator model under non-uniform pollution conditions. *IEEE Trans. Dielectr. Electr. Insul.* **17**, 1284–1297 (2010).
- Faramarzi Palangar, M. & Mirzaie, M. Diagnosis porcelain and glass insulators conditions using phase angle index based on experimental test. *IEEE Trans. Dielectr. Electr. Insul.* **23**, 3–9 (2016).

27. Shaik, M. G. & Karuppaiyan, V. Investigation of surface degradation of aged high temperature vulcanized (HTV) silicone rubber insulators. *Energies* **12**, 3769 (2019).
28. Palangar, M. F. *et al.* Identification of composite insulator criticality based on a new leakage current diagnostic index. *IEEE Trans. Instrum. Meas.* **70**, 1–10 (2021).
29. Zhao, S., Jiang, X., Zhang, Z., Hu, J. & Shu, L. Flashover voltage prediction of composite insulators based on the characteristics of leakage current. *IEEE Trans. Power Deliv.* **28**, 1699–1708 (2013).
30. Terrab, H. & Bayadi, A. Experimental study using design of experiment of pollution layer effect on insulator performance taking into account the presence of dry bands. *IEEE Trans. Dielectr. Electr. Insul.* **21**, 2486–2495 (2014).
31. Liu, Y. & Du, B. X. Recurrent plot analysis of leakage current on flashover performance of rime-iced composite insulator. *IEEE Trans. Dielectr. Electr. Insul.* **17**, 465–472 (2010).
32. Li, J., Sima, W., Sun, C. & Sebo, S. A. Use of leakage currents of insulators to determine the stage characteristics of the flashover process and contamination level prediction. *IEEE Trans. Dielectr. Electr. Insul.* **17**, 490–501 (2010).
33. Ghosh, R., Chatterjee, B. & Chakravorti, S. A novel leakage current index for the field monitoring of overhead insulators under harmonic voltage. *IEEE Trans. Industr. Electron.* **65**, 1568–1576 (2018).
34. Kordkheili, H. H., Abravesh, H., Tabasi, M., Dakhem, M. & Abravesh, M. M. Determining the probability of flashover occurrence in composite insulators by using leakage current harmonic components. *IEEE Trans. Dielectr. Electr. Insul.* **17**, 502–512 (2010).
35. IEC 507, CEI Artificial pollution tests on high-voltage insulators to be used on A.C. systems. *Int. Stand.* **2**, 1–7 (1991).
36. Salem, A. A. *et al.* Proposal of a dynamic numerical approach in predicting flashover critical voltage. *Int. J. Power Electron. Drive Syst.* **10**, 602–610 (2019).
37. Salem, A. A. *et al.* Pollution flashover under different contamination profiles on high voltage insulator: Numerical and experiment investigation. *IEEE Access* **9**, 37800–37812 (2021).
38. Arshad, A. J., Tahir, A., Stewart, B. G. & Nekahi, A. Forecasting flashover parameters of polymeric insulators under contaminated conditions using the machine learning technique. *Energies* **15**, 3889 (2020).
39. Krzma, A. S., Albano, M., & Haddad, A. Flashover influence of fog rate on the characteristics of polluted silicone-rubber insulators. 2017 52nd International Universities Power Engineering Conference (UPEC), 1–5 (2017).
40. Zhang, Z., Qiao, X., Yang, S. & Jiang, X. Non-uniform distribution of contamination on composite insulators in HVDC transmission lines. *Appl. Sci.* **10**, 1962 (2018).
41. Aydogan, A., Atalar, F., Ersoy Yilmaz, A. & Rozga, P. Using the method of harmonic distortion analysis in partial discharge assessment in mineral oil in a non-uniform electric field. *Energies* **13**, 4830 (2020).
42. Fielding, A. H. & Bell, J. F. A review of methods for the assessment of prediction errors in conservation presence/absence models. *Environ. Conserv.* **24**, 38–49 (1997).
43. Ouchen, L., Bayadi, A. & Boudissa, R. Dynamic model to predict the characteristics of the electric arc around a polluted insulator. *IET Sci. Meas. Technol.* **14**, 83–90 (2019).
44. Liu, Y. *et al.* Feature extraction and classification of surface discharges on an ice-covered insulator string during AC flashover using gray-level co-occurrence matrix. *Sci. Rep.* **11**, 2542 (2021).
45. Dong, B. *et al.* AC flashover voltage model for polluted suspension insulators and an experimental investigation in salt fog. *IEEE Access* **8**, 187411–187418 (2020).

Acknowledgements

This work was supported by the Collaborative Research in Engineering, Science, and Technology (CREST) under Grant 304/PELECT/6050424/C121 and Universiti Sains Malaysia Research University (RU) under Grant 1001/PELECT/8014097 and the Post-Doctoral Fellowship Scheme under the Professional Development Research University Grant (05E68) from Universiti Teknologi Malaysia.

Author contributions

A.A.S., K.Y.L., W.R. and Z.A.-M. conceived the experiments. A.A.S., K.Y.L., S.A.A.-G., R.A.R. and S.A.-A. conducted the experiments, and A.A.S., K.Y.L., W.R., Z.A.-M., S.A.A.-G., R.A.R. and S.A.-A. performed statistical analysis and figure generation. All authors reviewed the manuscript.

Competing interests

The authors declare no competing interests.

Additional information

Supplementary Information The online version contains supplementary material available at <https://doi.org/10.1038/s41598-022-17792-x>.

Correspondence and requests for materials should be addressed to A.A.S., K.Y.L. or W.R.

Reprints and permissions information is available at www.nature.com/reprints.

Publisher's note Springer Nature remains neutral with regard to jurisdictional claims in published maps and institutional affiliations.



Open Access This article is licensed under a Creative Commons Attribution 4.0 International License, which permits use, sharing, adaptation, distribution and reproduction in any medium or format, as long as you give appropriate credit to the original author(s) and the source, provide a link to the Creative Commons licence, and indicate if changes were made. The images or other third party material in this article are included in the article's Creative Commons licence, unless indicated otherwise in a credit line to the material. If material is not included in the article's Creative Commons licence and your intended use is not permitted by statutory regulation or exceeds the permitted use, you will need to obtain permission directly from the copyright holder. To view a copy of this licence, visit <http://creativecommons.org/licenses/by/4.0/>.

© The Author(s) 2022